

**HHS PUBLIC ACCESS**

Author manuscript

Brain Struct Funct. Author manuscript; available in PMC 2016 January 23.

Published in final edited form as:

Brain Struct Funct. 2016 January ; 221(1): 447–461. doi:10.1007/s00429-014-0917-3.**Cortical thickness and surface area in neonates at high risk for schizophrenia****Gang Li,**

Department of Radiology and BRIC, University of North Carolina at Chapel Hill, Chapel Hill, NC 27154, USA. Radiology and BRIC, UNC-CH School of Medicine, MRI Building, CB #7513 106 Mason Farm Road, Chapel Hill, NC 27599, USA

Li Wang,

Department of Radiology and BRIC, University of North Carolina at Chapel Hill, Chapel Hill, NC 27154, USA

Feng Shi,

Department of Radiology and BRIC, University of North Carolina at Chapel Hill, Chapel Hill, NC 27154, USA

Amanda E. Lyall,

Department of Psychiatry, University of North Carolina at Chapel Hill, Chapel Hill, NC 27154, USA

Mihye Ahn,

Department of Biostatistics and BRIC, University of North Carolina at Chapel Hill, Chapel Hill, NC 27154, USA

Ziwen Peng,

Department of Radiology and BRIC, University of North Carolina at Chapel Hill, Chapel Hill, NC 27154, USA

Hongtu Zhu,

Department of Biostatistics and BRIC, University of North Carolina at Chapel Hill, Chapel Hill, NC 27154, USA

Weili Lin,

Department of Radiology and BRIC, University of North Carolina at Chapel Hill, Chapel Hill, NC 27154, USA

John H. Gilmore, and

Department of Psychiatry, University of North Carolina at Chapel Hill, Chapel Hill, NC 27154, USA

Dinggang Shen

Correspondence to: Dinggang Shen, dgshen@med.unc.edu.

Electronic supplementary material The online version of this article (doi:10.1007/s00429-014-0917-3) contains supplementary material, which is available to authorized users.

Conflict of interest All authors report no potential conflicts of interest.

Department of Radiology and BRIC, University of North Carolina at Chapel Hill, Chapel Hill, NC 27154, USA. Radiology and BRIC, UNC-CH School of Medicine, MRI Building, CB #7513 106 Mason Farm Road, Chapel Hill, NC 27599, USA. Department of Brain and Cognitive Engineering, Korea University, Seoul, Republic of Korea

Gang Li: gang_li@med.unc.edu; Dinggang Shen: dgshen@med.unc.edu

Abstract

Schizophrenia is a neurodevelopmental disorder associated with subtle abnormal cortical thickness and cortical surface area. However, it is unclear whether these abnormalities exist in neonates associated with genetic risk for schizophrenia. To this end, this preliminary study was conducted to identify possible abnormalities of cortical thickness and surface area in the high-genetic-risk neonates. Structural magnetic resonance images were acquired from offspring of mothers ($N = 21$) who had schizophrenia ($N = 12$) or schizoaffective disorder ($N = 9$), and also matched healthy neonates of mothers who were free of psychiatric illness ($N = 26$). Neonatal cortical surfaces were reconstructed and parcellated as regions of interest (ROIs), and cortical thickness for each vertex was computed as the shortest distance between the inner and outer surfaces. Comparisons were made for the average cortical thickness and total surface area in each of 68 cortical ROIs. After false discovery rate (FDR) correction, it was found that the female high-genetic-risk neonates had significantly thinner cortical thickness in the right lateral occipital cortex than the female control neonates. Before FDR correction, the high-genetic-risk neonates had significantly thinner cortex in the left transverse temporal gyrus, left banks of superior temporal sulcus, left lingual gyrus, right paracentral cortex, right posterior cingulate cortex, right temporal pole, and right lateral occipital cortex, compared with the control neonates. Before FDR correction, in comparison with control neonates, male high-risk neonates had significantly thicker cortex in the left frontal pole, left cuneus cortex, and left lateral occipital cortex; while female high-risk neonates had significantly thinner cortex in the bilateral paracentral, bilateral lateral occipital, left transverse temporal, left pars opercularis, right cuneus, and right posterior cingulate cortices. The high-risk neonates also had significantly smaller cortical surface area in the right pars triangularis (before FDR correction), compared with control neonates. This preliminary study provides the first evidence that early development of cortical thickness and surface area might be abnormal in the neonates at genetic risk for schizophrenia.

Keywords

Schizophrenia; Schizoaffective disorder; High-risk; Neonates; Cortical surface area; Cortical thickness

Introduction

Schizophrenia is a neurodevelopmental disorder (Rapoport et al. 2005), characterized by hallucinations, delusions, and cognitive deficits, with heritability estimated at up to 80 % (Purcell et al. 2009). The first onset of psychosis in schizophrenia usually emerges in the late adolescence or early adulthood (Insel 2010), which is the end result of decades of interaction between genetic and environmental factors (Ross 2010). The early infancy period is one critical window, during which vulnerability is established; while the adolescent or young

adult period is the other critical window, during which the conversion from vulnerability to psychosis occurs (Ross 2010). Longitudinal studies have shown evidence of abnormalities preceding symptom onset, including delayed developmental milestone in their first year of life in adults with schizophrenia (Sorensen et al. 2010), and reduced IQ in children who destined to develop schizophrenia (Reichenberg et al. 2010; Woodberry et al. 2008). Having an affected relative also increases the risk for schizophrenia. For example, 20–50 % of children born to schizophrenic mothers exhibit developmental abnormalities (Marcus et al. 1993). Their risk of developing schizophrenia is about 10 times higher than that of the normal population (Sullivan 2005). High-risk neonates born to schizophrenic mothers, with the minimal exposure to environmental influences, are ideal candidates for increasing our understanding of brain changes associated with vulnerability to later to schizophrenia.

Magnetic resonance (MR) imaging studies have consistently found that schizophrenia is associated with the widespread cortical thinning, particularly affecting the prefrontal and temporal cortices in the first-episode and chronic subjects (Kuperberg et al. 2003; Narr et al. 2005a; Rimol et al. 2012), as well as reductions of the marginal cortical surface area (Rimol et al. 2012; Gutierrez-Galve et al. 2010). Unaffected relatives of individuals with schizophrenia have also been shown to exhibit cortical thickness abnormalities (Goghari et al. 2007b; Gogtay et al. 2007). Healthy relatives of schizophrenia patients show reduced cingulate thickness (Goghari et al. 2007b) and sulcal thickness alterations in the cingulate sulcus and superior temporal sulcus (Goghari et al. 2007a), and young healthy siblings of schizophrenia with childhood-onset schizophrenia exhibit thinner cortices in the temporal and prefrontal regions (Gogtay et al. 2007), though these are not the consistent findings (Goldman et al. 2009). In addition, adolescents at ultra-high risk for psychosis exhibit more cortical thinning in the left middle temporal cortex than controls (Ziermans et al. 2012). Young adults at genetic risk for schizophrenia also show low cortical thickness in the right anterior cingulate cortex, left paracingulate and posterior cingulate regions, bilateral frontal regions, temporal regions, inferior parietal and occipital regions (Byun et al. 2012). However, it remains unclear when the abnormalities of cortical thickness or surface area arise in patients with schizophrenia or their unaffected first-degree relatives.

Recent MR imaging studies of neonates at high genetic risk for schizophrenia have revealed structural abnormalities in the lateral ventricle, total gray matter (GM), cerebrospinal fluid, and intracranial volumes in male neonates (Gilmore et al. 2010a). Altered brain structural network was also found in high-risk neonates (Shi et al. 2012). These results suggest that the cortex developmental abnormalities in high-risk subjects may occur as early as the neonatal stage. Due to the low tissue contrast and high noise in the neonatal brain MR images, previous studies of high-risk neonates have been limited to the volume-based morphometric analyses. In fact, the cortical volume is the product of the cortical surface area and cortical thickness, which are driven by distinct cellular and genetic mechanisms (Panizzon et al. 2009; Chen et al. 2013). According to the radial unit hypothesis of cortical development, the cortical surface area is determined by the number of neuron columns that run perpendicular to the cortical surface, whereas the cortical thickness is influenced by the number of cells within a column (Rakic 1988). Therefore, volume-based morphometric analyses are unable to differentiate the cortex abnormality from either the cortical thickness or surface area, or both. With the recent advance in techniques for neonatal brain MR image processing (Wang

et al. 2011, 2013, 2014; Shi et al. 2010; Li et al. 2013a, 2014a), we are able to accurately reconstruct the neonatal cortical surfaces and further measure their cortical thickness and surface area, respectively, which is likely to provide more precise information of the possible cortex abnormalities. In this preliminary study, with our advanced infant-specific surface-based analysis pipeline (Li et al. 2013a, 2014a, b, c; Meng et al. 2014), for the first time, we are able to measure cortical thickness and surface area of neonates at high genetic risk for schizophrenia and matched control neonates, to identify whether the abnormalities of cortical thickness or surface area may exist in the high-risk neonates.

Materials and methods

Participants and MR image acquisition

The Institutional Review Board of the University of North Carolina (UNC) School of Medicine approved this study. Pregnant mothers with a confirmed diagnosis of schizophrenia or schizoaffective disorder were recruited and underwent a Structured Clinical Interview for DSM-IV Axis I Disorders (SCID) (Gilmore et al. 2010a). Past psychiatric records were obtained and a final consensus diagnosis was assigned. Matched control infants were selected from a companion study of normal brain development at UNC (Knickmeyer et al. 2008). Control infants were matched on gender, age in terms of time since last menstrual period at birth, age since the last menstrual period at MRI, and maternal age (Table 1). Potential control mothers were screened for psychiatric illness using a modified SCID. All genetic fathers and other first-degree relatives had no psychiatric illness, as confirmed by reports from children's mothers. The mean age of fathers was 30.8 ± 4.9 years. The dataset used in this paper has previously been used for studying brain volume differences and structural network difference between high-risk infants and control infants (Gilmore et al. 2010a; Shi et al. 2012).

All written informed consent forms were obtained from the parents. Exclusion criteria of infants included abnormalities on fetal ultrasound or major medical or psychotic illness in the mother. All infants were free of congenital anomalies, metabolic disease, and focal lesions. Detailed recruiting information can be found in Gilmore et al. (2010a) and Shi et al. (2012). Structural MR images were acquired from offspring of mothers ($N = 21$) who had schizophrenia ($N = 12$) or schizoaffective disorder ($N = 9$), and also matched healthy neonates of mothers who were free of psychiatric illness ($N = 26$).

MR images were acquired on a Siemens head-only 3T scanner with a circular polarized head coil. For T1-weighted images, 160 axial slices were obtained using the 3-dimensional magnetization-prepared rapid gradient-echo sequence: TR = 1,820 ms, TE = 4.38 ms, flip angle = 7° , and resolution = $1 \times 1 \times 1 \text{ mm}^3$. For T2-weighted MR images, 70 axial slices were acquired with turbo spin-echo sequences: TR = 7,380 ms, TE = 119 ms, flip angle = 150° , and resolution = $1.25 \times 1.25 \times 1.95 \text{ mm}^3$. The duration of T1 scan was 5:51 min, and the duration of T2 scan was 5:36 min. T2-weighted images were linearly aligned onto their respective T1-weighted images and further resampled to be $1 \times 1 \times 1 \text{ mm}^3$. Before scanning, infants were fed, swaddled, and fitted with ear protection. All infants were unsedated during scanning. Our current success rate for obtaining usable MRIs was approximately 90 % for neonates (Li et al. 2014c). All images in this study were visually checked and rated for

motion artifacts using a 4-point visual scale [none (1), mild (2), moderate (3), severe (4)] based on Blumenthal et al. (2002) and Lyall et al. (2014). The average motion artifact rating was less than 1.4.

Image processing

All MR images were preprocessed using the same infant-specific pipeline in Li et al. (2013a, b), including: (1) skull stripping, followed by manual editing to ensure the accurate removal of non-brain tissues; (2) removal of the cerebellum and brain stem; (3) correction of intensity inhomogeneity; (4) rigid alignment of all images onto the neonatal brain atlas (Shi et al. 2011). Tissue segmentation of neonatal brain MR images into gray matter (GM), white matter (WM) and cerebrospinal fluid (CSF) was performed by an infant-specific patch-driven coupled level sets method (Wang et al. 2013). After tissue segmentation, non-cortical structures were masked and filled, and each brain was separated into left and right hemispheres.

Based on tissue segmentation results, topologically correct and geometrically accurate cortical surfaces of each hemisphere for each subject were reconstructed using a deformable surface method (Li et al. 2012, 2014a). Specifically, the WM of each hemisphere was first topologically corrected to ensure having a spherical topology, and then the corrected WM was tessellated to form a triangulated surface mesh. Lastly, the triangular surface mesh of each hemisphere was deformed towards the reconstruction of the inner, central and outer cortical surfaces by preserving its initial topology. Note that the reconstructed cortical surfaces were spatially smooth and not constrained to voxel grids, thus achieving submillimeter accuracy (Li et al. 2014a). All inner cortical surfaces, with vertex-to-vertex correspondences to the outer cortical surfaces, were smoothed, inflated, and mapped to the standard sphere (Fischl et al. 1999). Each cortical surface was parcellated into 34 gyral-based regions of interest (ROIs) using Free-Surfer (Desikan et al. 2006). The cortical surface reconstruction and parcellation results were visually inspected for accuracy and further manually edited when needed. As major cortical folding is established at term birth and preserved during postnatal development (Li et al. 2013a, 2014c), the adult-based surface atlases in FreeSurfer, which encode major cortical folding information, achieve reasonable accuracy for parcellation of infant cortical surfaces (Li et al. 2013b), however, infant age-specific surface atlases would further improve the parcellation accuracy. The cortical thickness for each vertex was computed as the average value of the minimum distance from inner to outer surfaces and the minimum distance from outer to inner surfaces (Li et al. 2014a), similar to Fischl and Dale (2000). The mean cortical thickness value for each cortical region was then computed. The total surface area for each cortical region was computed based on the central cortical surface, which was defined as the surface lying in the geometric center between the inner and outer surfaces, for providing a balanced representation of gyral and sulcal regions (Van Essen 2005). The automated cortical surface measure computation results have been validated on five neonates with manual segmentation by a single rater. Intra-class correlations were calculated for regional cortical thickness and surface area, with the average value of 0.87 for cortical thickness and 0.91 for surface area, respectively (Lyall et al. 2014). Figure 1 shows the cortical surface reconstruction and parcellation results of a representative neonate.

Statistical analysis

To compare control and high-risk groups, we performed analysis of covariance (ANCOVA) procedure (Montgomery 2013). In this study, all analyses were implemented in SAS 9.3 software (SAS Institute, Cary NC) using generalized linear model (GENMOD) procedure to fit the ANCOVA. For each cortical region, we fit the following model

$$y_i = \beta_0 + \beta_1 \text{age}_i + \beta_2 \text{group}_i + \beta_3 \text{gender}_i + \beta_4 \text{group}_i \times \text{gender}_i + \beta_5 \text{birthage}_i + \varepsilon_i,$$

where, the subscript i represents the i th subject, y_i is the mean cortical thickness or total surface area, age_i is the gestational age in days at MRI acquisition, birthage_i is the gestational age in days at birth, group_i is 0 if control group and 1 if high-risk group, gender_i is 0 if male and 1 if female, and ε_i is an error term. For each ROI, we computed the least squares (LS) means and their standard errors (SE) for control and risk groups. By testing the differences of LS means between two groups, we obtained the z values and the corresponding p values. For each gender, we then followed the same procedure. Unless otherwise stated, p values were not corrected for multiple comparisons, as this study is primarily exploratory, hypothesis generating, and in need of replication.

Results

Cortical thickness

The mean cortical thickness and their SE of each group were provided in Table 2. No significant group difference was found between infants at high genetic risk for schizophrenia and the control infants on mean cortical thickness of left or right hemisphere. ROI-based analysis revealed that there were significant group differences between the genetically high-risk infants and the control infants on the cortical thickness of the left transverse temporal gyrus ($p = 0.009$), left banks of superior temporal sulcus ($p = 0.035$), left lingual gyrus ($p = 0.019$), right lateral occipital cortex ($p = 0.014$), right paracentral cortex ($p = 0.017$), right posterior cingulate cortex ($p = 0.041$), and right temporal pole ($p = 0.042$), with the high-risk infants having thinner cortical thickness than the control infants (Table 3). In addition, the left frontal pole exhibited significantly larger cortical thickness in the high-risk infants ($p = 0.048$), compared with the control infants. Scatterplots of the mean cortical thickness in these ROIs are shown in Fig. 2a.

ROI-based subgroup analysis further revealed strong group differences. The male high-risk infants had significantly thicker cortical thickness in the left frontal pole ($p = 0.014$), left cuneus cortex ($p = 0.002$), and left occipital cortex ($p = 0.043$) than the male control infants (Table S1; Fig. 2b). In addition, the male high-risk infants also had significantly thinner cortical thickness in the right temporal pole ($p = 0.002$) than the male control infants. The female high-risk infants had significantly thinner cortical thickness in the left paracentral ($p = 0.033$), right paracentral ($p = 0.002$), left lateral occipital ($p = 0.010$), right lateral occipital ($p = 0.0004$), left pars opercularis ($p = 0.013$), left transverse temporal ($p = 0.028$), right cuneus ($p = 0.037$), and right posterior cingulate ($p = 0.034$) cortices than the female control infants (Table S2; Fig. 2c). The right lateral occipital cortex remained significant even after

multiple comparison correction (FDR corrected $p = 0.028$). In addition, the female high-risk infants had significantly thicker cortical thickness in the right medial orbitofrontal frontal cortex ($p = 0.046$) than the female control infants. However, group \times gender interaction effects (for testing whether two groups have different cortical thickness for both genders) were only found to be significant in the left cuneus cortex ($p = 0.001$), right cuneus cortex ($p = 0.022$), left lateral occipital cortex ($p = 0.002$), right lateral occipital cortex ($p = 0.034$), and right temporal pole ($p = 0.009$).

Cortical surface area

The total cortical surface area and the SE of each group were provided in Table 4. No significant group difference was found between the high-risk infants and control infants on the total surface areas of left and right hemispheres. ROI-based group analysis found significantly smaller surface area in the right pars triangularis ($p = 0.028$) in the high-risk infants, compared with the control infants (Table 5; Fig. 3a). Subgroup analysis further revealed strong group differences on regional surface area. Specifically, male high-risk infants exhibited significantly smaller surface area in the right pars triangularis ($p = 0.032$) and right fusiform gyrus ($p = 0.026$), compared with the male control infants (Table S3; Fig. 3b). In contrast, no significant difference was found between female high-risk infants and female control infants on the surface area in any ROI (Table S4). However, group \times gender interaction effect was only significant in the right fusiform gyrus ($p = 0.007$).

Discussion

This is the first preliminary study investigating the cortical thickness and surface area separately in the neonates at high genetic risk for schizophrenia. Previous imaging morphometric studies of high-risk neonates have focused on measurement of brain volumes, which is unable to differentiate the possible cortex abnormality from either the cortical thickness or surface area, or both. With the state-of-the-art methods for neonatal brain MRI segmentation and cortical surface reconstruction (Wang et al. 2013; Li et al. 2014a), for the first time, we are able to accurately compute the cortical thickness and surface area, and perform advanced surface-based analysis of the whole cortex in neonates. The cortical surface-based analysis is particularly appropriate for studying the highly convoluted cortical structures than volume-based morphometric methods, as it respects the topology of the cortex and facilitates alignment, analysis and visualization of buried cortical regions (Van Essen 2005; Fischl et al. 1999).

We found that the female high-risk neonates had significantly thinner cortical thickness in the right lateral occipital cortex than the female control neonates after multiple comparisons correction. In the high-risk adult subjects, the reduced cortical thickness in the occipital cortex has been found (Byun et al. 2012), although previous studies of both high-risk adults and healthy siblings of schizophrenia have mainly found the reduced cortical thickness or volume in the prefrontal and temporal regions (Thermenos et al. 2013). In addition, cortical thinning in the occipital cortex has also been found in the first-episode schizophrenia (Narr et al. 2005b; Sprooten et al. 2013), and also smaller GM volumes in the occipital lobe were exhibited in the schizophrenia patients with good outcomes than the patients with poor

outcomes (Mitelman et al. 2003). Moreover, visual processing abnormalities have also been found in schizophrenia (Butler et al. 2008), and the abnormal neuronal density has been shown in the occipital cortex in postmortem schizophrenic brains (Selemon et al. 1995). Our finding provides the first evidence that cortical thickness may be abnormal in the neonates at high genetic risk for schizophrenia. The abnormal cortical thickness in the high-risk neonates may potentially reflect abnormalities of neuronal migration and mini-columnar formation for the cortex during gestation (Keshavan and Hogarty 1999). However, as children of parents with schizophrenia are at high risk, not only for schizophrenia but also for a variety of psychiatric disorders, including attention-deficit/hyper-activity, anxiety disorders, and depression (Ross and Compagnon 2001; Keshavan et al. 2008), our finding most likely reflects the genetic liability, or a genetic effect relevant to early brain development.

Before correction of multiple comparisons, we found more additional significant regions. For example, high-risk neonates had significantly thinner cortical thickness in the temporal cortex, including the left transverse temporal gyrus (Heschl's gyrus, primary auditory cortex), left superior temporal sulcus, and right temporal pole. Our findings are generally consistent with the existing finding in the healthy siblings and high-risk subjects of schizophrenia. For example, young healthy siblings of patients with childhood-onset schizophrenia showed significant GM deficits in the bilateral temporal cortices, compared with the controls (Gogtay et al. 2007). The adult unaffected siblings of schizophrenia patients showed GM decreases in the superior temporal cortex (but not significant after correction for multiple comparisons) (Honea et al. 2008). Young individuals at high familial risk for schizophrenia showed significant cortical thinning in the left middle temporal gyrus (Sprooten et al. 2013). In the adults, cortical thinning in the Heschl's gyrus has been found in the genetically high-risk subjects for schizophrenia (Byun et al. 2012). Reduced cortical thickness in the superior temporal sulcus was also found in the genetically high-risk adults (Gogtay et al. 2007), and reduced superior temporal gyral volume was found in young offspring of patients with schizophrenia (Rajarethinam et al. 2004). In addition, our finding of cortical thinning in the lingual gyrus in high-risk neonates was also consistent with the findings in high-risk adults (Byun et al. 2012). Our result was consistent with the hypothesis that the early infancy period is one critical window, during which vulnerability is established (Ross 2010; Thermenos et al. 2013).

Note that there might exist dynamic interactions across time and vulnerable regions. During the first 2 years of life, the cerebral cortex exhibits the regionally heterogeneous and dynamic development (Gilmore et al. 2012; Hanson et al. 2013; Nie et al. 2012, 2013; Knickmeyer et al. 2008; Li et al. 2013a; Lyall et al. 2014; Yap et al. 2011), due to the rapid growth of synaptic connections and dendritic complexity, abnormalities of which have been shown in postmortem studies in schizophrenia (Glantz and Lewis 2000; Black et al. 2004). At term birth, the cortical thickness in the prefrontal and temporal regions is less matured than that in the occipital cortex (Lyall et al. 2014). During this critical developmental stage, the prefrontal and temporal regions exhibit the most dynamic cortical thickness growth, while the occipital cortex exhibits the least amount of cortical thickness growth (Lyall et al. 2014). Moreover, multiple genes contribute to risk for schizophrenia (Aberg et al. 2013), and also genetic effects on the cortex development increase with the age in infants (Gilmore

et al. 2010b). Therefore, cortical thickness alterations in the high-risk neonates might become evident or shown in other regions, e.g., the prefrontal cortex, during the brain development in this stage. Studying the longitudinal developmental trajectories of the cortical thickness in these high-risk neonates will further critically increase our understanding of schizophrenia.

Subgroup analysis revealed significant gender effects (before correction of multiple comparisons), with the male high-risk neonates having thicker cortical thickness than the male control neonates in the left frontal pole, cuneus cortex, and lateral occipital cortex; while the female high-risk neonates had significantly thinner cortex than the female control neonates in bilateral paracentral, bilateral lateral occipital, left transverse temporal, left pars opercularis, right cuneus, and right posterior cingulate cortices. Our previous study found that neonatal males at risk for schizophrenia had larger brain volume and about 6 % larger cortical GM volume, compared to the controls (Gilmore et al. 2010a). Several cortical regions did show larger cortical thickness in high-risk male neonates, and the left hemisphere had quantitatively larger cortical thickness, which is consistent with the previous findings (Gilmore et al. 2010a). Note that the image processing for each analysis was different (surface-based vs volume-based), which may explain the differences between the studies.

We found significantly smaller surface area in the right pars triangularis in high-risk neonates (before multiple comparisons correction). In the adolescent high-risk studies, this region has shown significant reduction of the cortical surface area in 1-year follow-up (Prasad et al. 2010). Our results are consistent with findings with other schizophrenia studies of high-risk subjects and patients that the reduction in cortical volume was mainly driven by cortical thinning, although marginal surface area reduction had also been found in the circumscribed regions (Rimol et al. 2012; Gutierrez-Galve et al. 2010; Thermenos et al. 2013). In addition, our results are also consistent with the cortex developmental theory that the cortical surface area and cortical thickness are driven by distinct cellular and genetic mechanisms (Panizzon et al. 2009; Chen et al. 2013).

In this study, we mixed the schizophrenia and schizoaffective disorder, which differs from schizophrenia in terms of the presence of distinct mood episodes. In the previous studies, schizoaffective probands were often intermingled with schizophrenia case subjects and showed similar GM characteristics (Cannon et al. 1998; Radonic et al. 2011). For example, schizophrenia and schizoaffective probands showed overlapping GM reductions in numerous cortical and subcortical regions (Ivleva et al. 2013). However, it should be noted that, mixing schizophrenia and schizoaffective disorder may run at risk of mixing two disorders, which might have substantially different genetic architectures.

This preliminary study has several limitations. First, given the heterogeneity of schizophrenia and schizoaffective disorder, the sample size in this study is limited due to the difficulty in recruiting pregnant mothers with schizophrenia and their infants and also the difficulty in imaging high-risk infants (Gilmore et al. 2010a). Large sample size and longitudinal studies are expected to further confirm the findings. Second, as the fathers are young (30.8 ± 4.9 years of age), it is possible that fathers may have developed schizophrenia

subsequent to the study. This would have an effect of increasing the genetic loading risk of the child. Third, high-risk infants were more likely to be exposed to medications such as antipsychotics, anti-depressants, and cigarette smoking, as well as alcohol during pregnancy. Previous studies have shown that the use of antipsychotics during pregnancy does not appear to significantly increase the risk of birth defects and other adverse outcomes (Einarson and Boskovic 2009), although the influence of antipsychotics on prenatal cortex development is unclear. Brain volume studies do not find significant differences between the high-risk neonates exposed to maternal cigarette smoking and those who were not exposed (Gilmore et al. 2010a). Prenatal exposure to maternal cigarette smoking has been shown to cause the thinner orbitofrontal, middle frontal, and parahippocampal cortices in adolescents (Toro et al. 2008; Lotfipour et al. 2009). Previous studies have also shown that children and the youth with heavy prenatal alcohol exposure have thicker cortical thickness in the frontal, temporal, and parietal regions than the control subjects (Sowell et al. 2008; Yang et al. 2012). All these factors could have confounded the results. Fourth, high-risk infants born to schizophrenic mothers are likely to be in worse living conditions, such as poor nutrition. This could also have confounded the results. Lastly, the majority of individuals born with vulnerability will never develop the full clinical disorder (Ross 2010). Although cortical thickness and surface area abnormalities may exist in the high-risk neonates, only 10 % among them are expected to ultimately develop schizophrenia (Gilmore et al. 2010a).

In summary, using the infant-specific cortical surface-based morphometry, this preliminary study provides the first evidence of possible abnormal cortical thickness and surface area development in the high-risk neonatal subjects. This suggests the possible need of early identification, prevention, and intervention strategies for schizophrenia (and other psychiatric disorders) to target this critical period of early brain development.

Acknowledgments

The authors would like to thank the editor and anonymous reviewers for providing constructive and detailed suggestions that have improved this paper significantly. This work was supported in part by National Institutes of Health (grant numbers EB006733, EB008760, EB008374, EB009634, MH088520, MH070890, MH064065, MH100217, NS055754, and HD053000).

References

- Aberg KA, Liu Y, Bukszar J, McClay JL, Khachane AN, Andreassen OA, Blackwood D, Corvin A, Djurovic S, Gurling H, Ophoff R, Pato CN, Pato MT, Riley B, Webb T, Kendler K, O'Donovan M, Craddock N, Kirov G, Owen M, Rujescu D, St Clair D, Werge T, Hultman CM, Delisi LE, Sullivan P, van den Oord EJ. A comprehensive family-based replication study of schizophrenia genes. *JAMA Psychiatry*. 2013; 70(2):1–9. [PubMed: 23925710]
- Black JE, Kodish IM, Grossman AW, Klintsova AY, Orlovskaya D, Vostrikov V, Uranova N, Greenough WT. Pathology of layer V pyramidal neurons in the prefrontal cortex of patients with schizophrenia. *Am J Psychiatry*. 2004; 161(4):742–744. [PubMed: 15056523]
- Blumenthal JD, Zijdenbos A, Molloy E, Giedd JN. Motion artifact in magnetic resonance imaging: implications for automated analysis. *Neuroimage*. 2002; 16(1):89–92. [PubMed: 11969320]
- Butler PD, Silverstein SM, Dakin SC. Visual perception and its impairment in schizophrenia. *Biol Psychiatry*. 2008; 64(1):40–47. [PubMed: 18549875]
- Byun MS, Kim JS, Jung WH, Jang JH, Choi JS, Kim SN, Choi CH, Chung CK, An SK, Kwon JS. Regional cortical thinning in subjects with high genetic loading for schizophrenia. *Schizophr Res*. 2012; 141(2–3):197–203. [PubMed: 22998933]

- Cannon TD, van Erp TGM, Huttunen M, Lonnqvist J, Salonen O, Valanne L, Poutanen VP, Standertskjold-Nordenstam CG, Gur RE, Yan M. Regional gray matter, white matter, and cerebrospinal fluid distributions in schizophrenic patients, their siblings, and controls. *Arch Gen Psychiatry*. 1998; 55(12):1084–1091. [PubMed: 9862551]
- Chen CH, Fiecas M, Gutierrez ED, Panizzon MS, Eyer LT, Vuoksima E, Thompson WK, Fennema-Notestine C, Hagler DJ Jr, Jernigan TL, Neale MC, Franz CE, Lyons MJ, Fischl B, Tsuang MT, Dale AM, Kremen WS. Genetic topography of brain morphology. *Proc Natl Acad Sci USA*. 2013; 110(42):17089–17094. [PubMed: 24082094]
- Desikan RS, Segonne F, Fischl B, Quinn BT, Dickerson BC, Blacker D, Buckner RL, Dale AM, Maguire RP, Hyman BT, Albert MS, Killiany RJ. An automated labeling system for subdividing the human cerebral cortex on MRI scans into gyral based regions of interest. *Neuroimage*. 2006; 31(3): 968–980. [PubMed: 16530430]
- Einarson A, Boskovic R. Use and safety of antipsychotic drugs during pregnancy. *J Psychiatr Pract*. 2009; 15(3):183–192. [PubMed: 19461391]
- Fischl B, Dale AM. Measuring the thickness of the human cerebral cortex from magnetic resonance images. *Proc Natl Acad Sci USA*. 2000; 97(20):11050–11055. [PubMed: 10984517]
- Fischl B, Sereno MI, Dale AM. Cortical surface-based analysis. II: inflation, flattening, and a surface-based coordinate system. *Neuroimage*. 1999; 9(2):195–207. [PubMed: 9931269]
- Gilmore JH, Kang C, Evans DD, Wolfe HM, Smith JK, Lieberman JA, Lin W, Hamer RM, Styner M, Gerig G. Prenatal and neonatal brain structure and white matter maturation in children at high risk for schizophrenia. *Am J Psychiatry*. 2010a; 167(9):1083–1091. [PubMed: 20516153]
- Gilmore JH, Schmitt JE, Knickmeyer RC, Smith JK, Lin W, Styner M, Gerig G, Neale MC. Genetic and environmental contributions to neonatal brain structure: a twin study. *Hum Brain Mapp*. 2010b; 31(8):1174–1182. [PubMed: 20063301]
- Gilmore JH, Shi F, Woolson SL, Knickmeyer RC, Short SJ, Lin W, Zhu H, Hamer RM, Styner M, Shen D. Longitudinal development of cortical and subcortical gray matter from birth to 2 years. *Cereb Cortex*. 2012; 22(11):2478–2485. [PubMed: 22109543]
- Glantz LA, Lewis DA. Decreased dendritic spine density on prefrontal cortical pyramidal neurons in schizophrenia. *Arch Gen Psychiatry*. 2000; 57(1):65–73. [PubMed: 10632234]
- Goghari VM, Rehm K, Carter CS, Macdonald AW. Sulcal thickness as a vulnerability indicator for schizophrenia. *Brit J Psychiatry*. 2007a; 191:229–233. [PubMed: 17766763]
- Goghari VM, Rehm K, Carter CS, MacDonald AW 3rd. Regionally specific cortical thinning and gray matter abnormalities in the healthy relatives of schizophrenia patients. *Cereb Cortex*. 2007b; 17(2): 415–424. [PubMed: 16547347]
- Gogtay N, Greenstein D, Lenane M, Clasen L, Sharp W, Gochman P, Butler P, Evans A, Rapoport J. Cortical brain development in nonpsychotic siblings of patients with childhood-onset schizophrenia. *Arch Gen Psychiatry*. 2007; 64(7):772–780. [PubMed: 17606811]
- Goldman AL, Pezawas L, Mattay VS, Fischl B, Verchinski BA, Chen Q, Weinberger DR, Meyer-Lindenberg A. Widespread reductions of cortical thickness in schizophrenia and spectrum disorders and evidence of heritability. *Arch Gen Psychiatry*. 2009; 66(5):467–477. [PubMed: 19414706]
- Gutierrez-Galve L, Wheeler-Kingshott CA, Altmann DR, Price G, Chu EM, Leeson VC, Lobo A, Barker GJ, Barnes TR, Joyce EM, Ron MA. Changes in the frontotemporal cortex and cognitive correlates in first-episode psychosis. *Biol Psychiatry*. 2010; 68(1):51–60. [PubMed: 20452574]
- Hanson JL, Hair N, Shen D, Shi F, Gilmore JH, Wolfe BL, Pollak SD. Family poverty affects the rate of human infant brain growth. *PLoS One*. 2013; 8(12):e80954. [PubMed: 24349025]
- Honea RA, Meyer-Lindenberg A, Hobbs KB, Pezawas L, Mattay VS, Egan MF, Verchinski B, Passingham RE, Weinberger DR, Callicott JH. Is gray matter volume an intermediate phenotype for schizophrenia? A voxel-based morphometry study of patients with schizophrenia and their healthy siblings. *Biol Psychiatry*. 2008; 63(5):465–474. [PubMed: 17689500]
- Insel TR. Rethinking schizophrenia. *Nature*. 2010; 468(7321):187–193. [PubMed: 21068826]
- Ivleva EI, Bidesi AS, Keshavan MS, Pearlson GD, Meda SA, Dodig D, Moates AF, Lu HZ, Francis AN, Tandon N, Schretlen DJ, Sweeney JA, Clementz BA, Tammimga CA. Gray matter volume as

- an intermediate phenotype for psychosis: bipolar-schizophrenia network on intermediate phenotypes (B-SNIP). *Am J Psychiatry*. 2013; 170(11):1285–1296. [PubMed: 24185241]
- Keshavan MS, Hogarty GE. Brain maturational processes and delayed onset in schizophrenia. *Dev Psychopathol*. 1999; 11(3):525–543. [PubMed: 10532623]
- Keshavan M, Montrose DM, Rajarethinam R, Diwadkar V, Prasad K, Sweeney JA. Psychopathology among offspring of parents with schizophrenia: relationship to premorbid impairments. *Schizophr Res*. 2008; 103(1–3):114–120. [PubMed: 18442896]
- Knickmeyer RC, Gouttard S, Kang C, Evans D, Wilber K, Smith JK, Hamer RM, Lin W, Gerig G, Gilmore JH. A structural MRI study of human brain development from birth to 2 years. *J Neurosci*. 2008; 28(47):12176–12182. [PubMed: 19020011]
- Kuperberg GR, Broome MR, McGuire PK, David AS, Eddy M, Ozawa F, Goff D, West WC, Williams SC, van der Kouwe AJ, Salat DH, Dale AM, Fischl B. Regionally localized thinning of the cerebral cortex in schizophrenia. *Arch Gen Psychiatry*. 2003; 60(9):878–888. [PubMed: 12963669]
- Li G, Nie J, Wu G, Wang Y, Shen D. Consistent reconstruction of cortical surfaces from longitudinal brain MR images. *Neuroimage*. 2012; 59(4):3805–3820. [PubMed: 22119005]
- Li G, Nie J, Wang L, Shi F, Lin W, Gilmore JH, Shen D. Mapping region-specific longitudinal cortical surface expansion from birth to 2 years of age. *Cereb Cortex*. 2013a; 23(11):2724–2733. [PubMed: 22923087]
- Li, G.; Wang, L.; Shi, F.; Lin, W.; Shen, D. Multi-atlas based simultaneous labeling of longitudinal dynamic cortical surfaces in infants. *Medical image computing and computer-assisted intervention —MICCAI 2013*. In: Mori, K.; Sakuma, I.; Sato, Y.; Barillot, C.; Navab, N., editors. *Lecture notes in computer science*. Vol. 8149. Springer; Berlin Heidelberg: 2013b. p. 58-65.
- Li G, Nie J, Wang L, Shi F, Gilmore JH, Lin W, Shen D. Measuring the dynamic longitudinal cortex development in infants by reconstruction of temporally consistent cortical surfaces. *Neuroimage*. 2014a; 90:266–279. [PubMed: 24374075]
- Li G, Nie J, Wang L, Shi F, Lyall AE, Lin W, Gilmore JH, Shen D. Mapping longitudinal hemispheric structural asymmetries of the human cerebral cortex from birth to 2 years of age. *Cereb Cortex*. 2014b; 24(5):1289–1300. [PubMed: 23307634]
- Li G, Wang L, Shi F, Lyall AE, Lin W, Gilmore JH, Shen D. Mapping longitudinal development of local cortical gyrification in infants from birth to 2 years of age. *J Neurosci*. 2014c; 34(12):4228–4238. [PubMed: 24647943]
- Lotfipour S, Ferguson E, Leonard G, Perron M, Pike B, Richer L, Seguin JR, Toro R, Veillette S, Pausova Z, Paus T. Orbitofrontal cortex and drug use during adolescence role of prenatal exposure to maternal smoking and BDNF genotype. *Arch Gen Psychiatry*. 2009; 66(11):1244–1252. [PubMed: 19884612]
- Lyall AE, Shi F, Geng X, Woolson S, Li G, Wang L, Hamer RM, Shen D, Gilmore JH. Dynamic development of regional cortical thickness and surface area in early childhood. *Cereb Cortex*. 2014.1093/cercor/bhu027
- Marcus J, Hans SL, Auerbach JG, Auerbach AG. Children at risk for schizophrenia: the Jerusalem Infant Development Study. II. Neurobehavioral deficits at school age. *Arch Gen Psychiatry*. 1993; 50(10):797–809. [PubMed: 7692835]
- Meng Y, Li G, Lin W, Gilmore JH, Shen D. Spatial distribution and longitudinal development of deep cortical sulcal landmarks in infants. *Neuroimage*. 2014; 100C:206–218. [PubMed: 24945660]
- Mitelman SA, Shihabuddin L, Brickman AM, Hazlett EA, Buchsbaum MS. MRI assessment of gray and white matter distribution in Brodmann's areas of the cortex in patients with schizophrenia with good and poor outcomes. *Am J Psychiatry*. 2003; 160(12):2154–2168. [PubMed: 14638586]
- Montgomery, DC. *Design and analysis of experiments*. 8. Wiley; Hoboken: 2013.
- Narr KL, Bilder RM, Toga AW, Woods RP, Rex DE, Szeszko PR, Robinson D, Sevy S, Gunduz-Bruce H, Wang YP, DeLuca H, Thompson PM. Mapping cortical thickness and gray matter concentration in first episode schizophrenia. *Cereb Cortex*. 2005a; 15(6):708–719. [PubMed: 15371291]

- Narr KL, Toga AW, Szeszko P, Thompson PM, Woods RP, Robinson D, Sevy S, Wang Y, Schrock K, Bilder RM. Cortical thinning in cingulate and occipital cortices in first episode schizophrenia. *Biol Psychiatry*. 2005b; 58(1):32–40. [PubMed: 15992520]
- Nie J, Li G, Wang L, Gilmore JH, Lin W, Shen D. A computational growth model for measuring dynamic cortical development in the first year of life. *Cereb Cortex*. 2012; 22(10):2272–2284. [PubMed: 22047969]
- Nie J, Li G, Shen D. Development of cortical anatomical properties from early childhood to early adulthood. *Neuroimage*. 2013; 76:216–224. [PubMed: 23523806]
- Panizzon MS, Fennema-Notestine C, Eyer LT, Jernigan TL, Prom-Wormley E, Neale M, Jacobson K, Lyons MJ, Grant MD, Franz CE, Xian H, Tsuang M, Fischl B, Seidman L, Dale A, Kremen WS. Distinct genetic influences on cortical surface area and cortical thickness. *Cereb Cortex*. 2009; 19(11):2728–2735. [PubMed: 19299253]
- Prasad KM, Goradia D, Eack S, Rajagopalan M, Nutche J, Magge T, Rajarethinam R, Keshavan MS. Cortical surface characteristics among offspring of schizophrenia subjects. *Schizophr Res*. 2010; 116(2–3):143–151. [PubMed: 19962858]
- Purcell SM, Wray NR, Stone JL, Visscher PM, O'Donovan MC, Sullivan PF, Sklar P. Common polygenic variation contributes to risk of schizophrenia and bipolar disorder. *Nature*. 2009; 460(7256):748–752. [PubMed: 19571811]
- Radonic E, Rados M, Kalember P, Bajsi-Janovic M, Folnegovic-Smalc V, Henigsberg N. Comparison of hippocampal volumes in schizophrenia, schizoaffective and bipolar disorder. *Collegium Antropol*. 2011; 35:249–252.
- Rajarethinam R, Sahni S, Rosenberg DR, Keshavan MS. Reduced superior temporal gyrus volume in young offspring of patients with schizophrenia. *Am J Psychiatry*. 2004; 161(6):1121–1124. [PubMed: 15169705]
- Rakic P. Specification of cerebral cortical areas. *Science*. 1988; 241(4862):170–176. [PubMed: 3291116]
- Rapoport JL, Addington AM, Frangou S, Psych MR. The neurodevelopmental model of schizophrenia: update 2005. *Mol Psychiatry*. 2005; 10(5):434–449. [PubMed: 15700048]
- Reichenberg A, Caspi A, Harrington H, Houts R, Keefe RS, Murray RM, Poulton R, Moffitt TE. Static and dynamic cognitive deficits in childhood preceding adult schizophrenia: a 30-year study. *Am J Psychiatry*. 2010; 167(2):160–169. [PubMed: 20048021]
- Rimol LM, Nesvag R, Hagler DJ Jr, Bergmann O, Fennema-Notestine C, Hartberg CB, Haukvik UK, Lange E, Pung CJ, Server A, Melle I, Andreassen OA, Agartz I, Dale AM. Cortical volume, surface area, and thickness in schizophrenia and bipolar disorder. *Biol Psychiatry*. 2012; 71(6):552–560. [PubMed: 22281121]
- Ross RG. Neuroimaging the infant: the application of modern neurobiological methods to the neurodevelopmental hypothesis of schizophrenia. *Am J Psychiatry*. 2010; 167(9):1017–1019. [PubMed: 20826850]
- Ross RG, Compagnon N. Diagnosis and treatment of psychiatric disorders in children with a schizophrenic parent. *Schizophr Res*. 2001; 50(1–2):121–129. [PubMed: 11378320]
- Selemon LD, Rajkowska G, Goldman-Rakic PS. Abnormally high neuronal density in the schizophrenic cortex. A morphometric analysis of prefrontal area 9 and occipital area 17. *Arch Gen Psychiatry*. 1995; 52(10):805–818. (discussion 819–820). [PubMed: 7575100]
- Shi F, Yap PT, Fan Y, Gilmore JH, Lin W, Shen D. Construction of multi-region-multi-reference atlases for neonatal brain MRI segmentation. *Neuroimage*. 2010; 51(2):684–693. [PubMed: 20171290]
- Shi F, Yap PT, Wu G, Jia H, Gilmore JH, Lin W, Shen D. Infant brain atlases from neonates to 1- and 2-year-olds. *PLoS One*. 2011; 6(4):e18746. [PubMed: 21533194]
- Shi F, Yap PT, Gao W, Lin W, Gilmore JH, Shen D. Altered structural connectivity in neonates at genetic risk for schizophrenia: a combined study using morphological and white matter networks. *Neuroimage*. 2012; 62(3):1622–1633. [PubMed: 22613620]
- Sorensen HJ, Mortensen EL, Schiffman J, Reinisch JM, Maeda J, Mednick SA. Early developmental milestones and risk of schizophrenia: a 45-year follow-up of the Copenhagen Perinatal Cohort. *Schizophr Res*. 2010; 118(1–3):41–47. [PubMed: 20181463]

- Sowell ER, Mattson SN, Kan E, Thompson PM, Riley EP, Toga AW. Abnormal cortical thickness and brain-behavior correlation patterns in individuals with heavy prenatal alcohol exposure. *Cereb Cortex*. 2008; 18(1):136–144. [PubMed: 17443018]
- Sprooten E, Pappmeyer M, Smyth AM, Vincenz D, Honold S, Conlon GA, Moorhead TW, Job D, Whalley HC, Hall J, McIntosh AM, Owens DC, Johnstone EC, Lawrie SM. Cortical thickness in first-episode schizophrenia patients and individuals at high familial risk: a cross-sectional comparison. *Schizophr Res*. 2013; 151(1–3):259–264. [PubMed: 24120958]
- Sullivan PF. The genetics of schizophrenia. *PLoS Med*. 2005; 2(7):e212. [PubMed: 16033310]
- Thermenos HW, Keshavan MS, Juelich RJ, Molokotos E, Whitfield-Gabrieli S, Brent BK, Makris N, Seidman LJ. A review of neuroimaging studies of young relatives of individuals with schizophrenia: a developmental perspective from schizotaxia to schizophrenia. *Am J Med Genet B*. 2013; 162(7):604–635.
- Toro R, Leonard G, Lerner JV, Lerner RM, Perron M, Pike GB, Richer L, Veillette S, Pausova Z, Paus T. Prenatal exposure to maternal cigarette smoking and the adolescent cerebral cortex. *Neuropsychopharmacology*. 2008; 33(5):1019–1027. [PubMed: 17609681]
- Van Essen DC. A population-average, landmark- and surface-based (PALS) atlas of human cerebral cortex. *Neuroimage*. 2005; 28(3):635–662. [PubMed: 16172003]
- Wang L, Shi F, Lin W, Gilmore JH, Shen D. Automatic segmentation of neonatal images using convex optimization and coupled level sets. *Neuroimage*. 2011; 58:805–817. [PubMed: 21763443]
- Wang L, Shi F, Li G, Gao Y, Lin W, Gilmore JH, Shen D. Segmentation of neonatal brain MR images using patch-driven level sets. *Neuroimage*. 2013; 84C:141–158. [PubMed: 23968736]
- Wang L, Shi F, Gao Y, Li G, Gilmore JH, Lin W, Shen D. Integration of sparse multi-modality representation and anatomical constraint for iso-intense infant brain MR image segmentation. *Neuroimage*. 2014; 89:152–164. [PubMed: 24291615]
- Woodberry KA, Giuliano AJ, Seidman LJ. Premorbid IQ in schizophrenia: a meta-analytic review. *Am J Psychiatry*. 2008; 165(5):579–587. [PubMed: 18413704]
- Yang Y, Roussotte F, Kan E, Sulik KK, Mattson SN, Riley EP, Jones KL, Adnams CM, May PA, O'Connor MJ, Narr KL, Sowell ER. Abnormal cortical thickness alterations in fetal alcohol spectrum disorders and their relationships with facial dysmorphology. *Cereb Cortex*. 2012; 22(5):1170–1179. [PubMed: 21799209]
- Yap PT, Fan Y, Chen Y, Gilmore JH, Lin W, Shen D. Development trends of white matter connectivity in the first years of life. *PLoS One*. 2011; 6(9):e24678. [PubMed: 21966364]
- Ziermans TB, Schothorst PF, Schnack HG, Koolschijn PC, Kahn RS, van Engeland H, Durston S. Progressive structural brain changes during development of psychosis. *Schizophr Bull*. 2012; 38(3):519–530. [PubMed: 20929968]

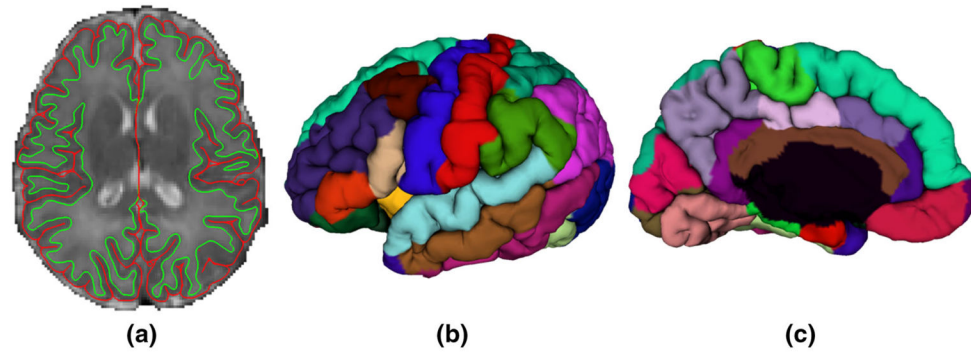


Fig. 1. Cortical surface reconstruction and parcellation of a representative neonate. **a** Is an axial slice of reconstructed inner (*green color*) and outer (*red color*) cortical surfaces overlaid on the T2 MR image. **b** and **c** Are the lateral and medial views of the parcellation of the outer surface on the *left* hemisphere

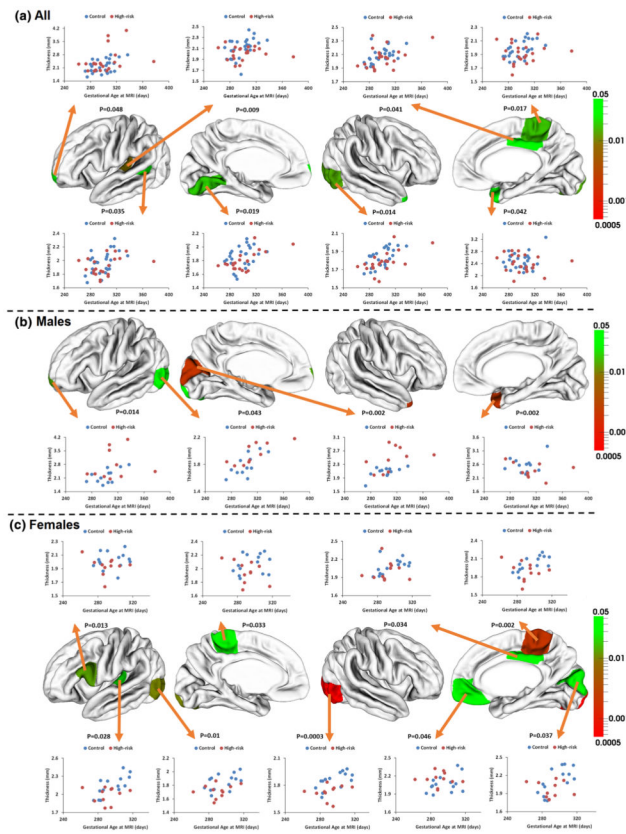


Fig. 2. *p* values and *scatterplots* of regional mean cortical thickness between infants at high genetic risk for schizophrenia and the control infants. The *color bar* of *p* values is provided on the right. *White colors* indicate non-significant regions

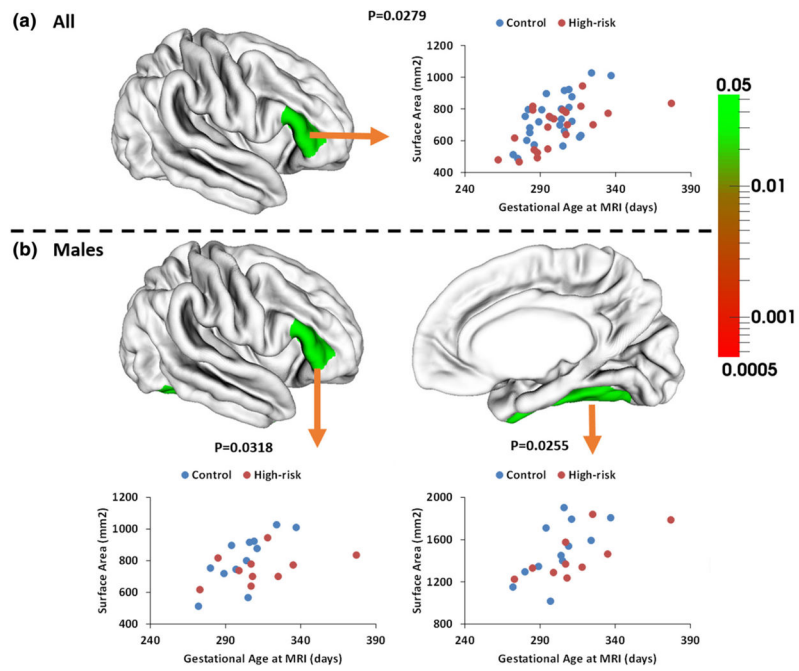


Fig. 3. *p* values and *scatterplots* of regional surface area between infants at high-risk for schizophrenia and the control infants. *White colors* indicate non-significant regions. No significant difference of regional surface area was found in two female groups

Table 1

Demographic characteristics, prenatal and perinatal conditions of infants at high genetic risk for schizophrenia and comparison infants

Characteristic, prenatal and perinatal condition ^a	Comparison infants (N = 26)		High-risk infants (N = 21)	
	N	%	N	%
Gender				
Male	12	46.2	10	47.6
Female	14	53.8	11	52.4
Ethnicity				
Caucasian	16	61.5	11	52.4
African American	10	38.5	10	47.6
Medication exposure				
Antipsychotic*	0	0.0	19	90.5
Antidepressant*	0	0.0	5	23.8
Lithium	0	0.0	2	9.5
Other medication	16	61.5	16	76.2
Substance exposure				
Tobacco smoking*	1	3.8	9	42.9
Alcohol	0	0.0	2	9.5
Marijuana	0	0.0	2	9.5
Cesarean section	7	26.9	8	38.1
Premature birth (< 37 weeks)	8	30.8	6	28.6
Stay in neonatal intensive care unit	2	7.7	6	28.6

	Mean	SD	Mean	SD
Maternal age (years)	28.1	3.7	27.3	3.9
Maternal education (years)*	13.9	2.9	10.0	3.5
Infant age (days since mother's last menstrual period)				
At birth	268.7	17.4	265.0	23.1
At MRI	299.0	16.2	300.7	24.8
Birth weight (g)	3,121	647.4	3,147.8	1,006.3
Apgar score ^b				
1 min	7.92	1.26	7.1	2.3
5 min	8.92	0.48	8.5	1.2

* Significant difference between groups ($p < 0.05$)

^a Detailed recruiting information can be referred to Gilmore et al. (2010a)

^b Apgar score is to assess the condition and prognosis of newborn infants, taken 1 and 5 min after birth. Apgar score ranges from 0 to 10, and neonates scoring 7 or above are generally considered in good health (Shi et al. 2012)

Table 2

Average cortical thickness of infants at high genetic risk for schizophrenia and control infants

	Control infants		High-risk infants		Difference (%)	<i>p</i> values
	Least squares mean	Standard error (SE)	Least squares mean	Standard error (SE)		
Left hemisphere	1.96	0.01	1.95	0.01	-0.47	0.631
Right hemisphere	1.93	0.01	1.91	0.01	-1.19	0.189
Male left hemisphere	1.95	0.02	1.97	0.02	0.86	0.565
Male right hemisphere	1.93	0.02	1.91	0.02	-1.07	0.445
Female left hemisphere	1.97	0.02	1.93	0.02	-1.79	0.158
Female right hemisphere	1.93	0.02	1.91	0.02	-1.31	0.267

Table 3
Regional cortical thickness of infants at high genetic risk for schizophrenia and control infants

Regions	Thickness (mm)		Difference (%)		p values
	Control infants		High-risk infants		
	Least squares mean	SE	Least squares mean	SE	
Frontal lobe					
Superior frontal left	2.06	0.02	2.06	0.03	0.14 0.9376
Superior frontal right	2.02	0.02	2.01	0.02	-0.64 0.6900
Rostral middle frontal left	1.98	0.03	2.01	0.03	1.13 0.5784
Rostral middle frontal right	1.94	0.02	1.96	0.02	1.34 0.4023
Caudal middle frontal left	1.90	0.02	1.90	0.02	-0.32 0.8476
Caudal middle frontal right	1.90	0.02	1.87	0.03	-1.44 0.4469
Pars opercularis left	1.99	0.02	1.95	0.02	-2.02 0.1300
Pars opercularis right	1.93	0.02	1.90	0.02	-1.57 0.2585
Pars triangularis left	2.07	0.03	2.06	0.04	-0.38 0.8705
Pars triangularis right	1.88	0.02	1.93	0.03	2.62 0.1820
Pars orbitalis left	2.06	0.03	2.08	0.04	0.73 0.7534
Pars orbitalis right	1.96	0.04	2.02	0.04	3.14 0.2566
Lateral orbital frontal left	1.93	0.02	1.94	0.02	0.42 0.7621
Lateral orbital frontal right	1.87	0.02	1.88	0.02	0.31 0.7990
Medial orbital frontal left	2.19	0.03	2.20	0.03	0.39 0.8336
Medial orbital frontal right	2.15	0.02	2.20	0.03	2.33 0.1851
Frontal pole left	2.21	0.08	2.45	0.09	10.70 0.0479*
Frontal pole right	2.17	0.06	2.29	0.06	5.39 0.1710
Precentral left	1.97	0.02	1.96	0.02	-0.88 0.5362
Precentral right	1.93	0.02	1.90	0.02	-1.77 0.1798
Paracentral left	2.05	0.02	2.00	0.03	-2.06 0.2532
Paracentral right	1.98	0.02	1.90	0.02	-3.86 0.0168*
Parietal lobe					
Postcentral left	1.96	0.02	1.96	0.02	0.08 0.9600
Postcentral right	1.89	0.02	1.85	0.02	-2.06 0.1370

Regions	Thickness (mm)		Difference (%)		p values
	Control infants		High-risk infants		
	Least squares mean	SE	Least squares mean	SE	
Supramarginal left	1.98	0.02	1.98	0.02	0.09 0.9579
Supramarginal right	1.93	0.02	1.90	0.02	-1.49 0.2690
Superior parietal left	1.88	0.02	1.87	0.02	-0.57 0.6803
Superior parietal right	1.88	0.02	1.86	0.02	-1.34 0.3089
Inferior parietal left	1.95	0.02	1.95	0.02	0.11 0.9360
Inferior parietal right	1.92	0.02	1.90	0.02	-1.13 0.3990
Precuneus left	1.99	0.01	1.97	0.02	-0.72 0.5014
Precuneus right	1.98	0.02	1.97	0.02	-0.70 0.5757
Temporal lobe					
Superior temporal left	2.06	0.02	2.06	0.02	0.27 0.8563
Superior temporal right	2.00	0.02	1.98	0.02	-1.01 0.4259
Middle temporal left	1.98	0.02	1.95	0.02	-1.51 0.3283
Middle temporal right	1.92	0.02	1.91	0.03	-0.81 0.6569
Inferior temporal left	1.94	0.02	1.87	0.03	-3.70 0.0516
Inferior temporal right	1.89	0.02	1.84	0.02	-2.63 0.1003
Transverse temporal left	2.12	0.03	2.00	0.03	-5.28 0.0088*
Transverse temporal right	2.16	0.04	2.12	0.04	-1.61 0.5157
Banks superior temporal sulcus left	1.98	0.02	1.90	0.03	-4.03 0.0354*
Banks superior temporal sulcus right	2.00	0.03	1.94	0.03	-3.12 0.1330
Entorhinal left	2.09	0.05	2.08	0.06	-0.59 0.8799
Entorhinal right	2.34	0.07	2.35	0.07	0.32 0.9401
Parahippocampal Left	1.66	0.03	1.71	0.03	2.97 0.2249
Parahippocampal Right	1.70	0.03	1.66	0.03	-2.32 0.3178
Temporal pole left	2.55	0.05	2.59	0.05	1.35 0.6387
Temporal pole right	2.51	0.04	2.38	0.05	-5.27 0.0416*
Fusiform left	1.74	0.02	1.70	0.02	-2.01 0.1297
Fusiform right	1.73	0.02	1.69	0.02	-2.22 0.1750
Occipital lobe					

Regions	Thickness (mm)		Difference (%)		p values
	Control infants		High-risk infants		
	Least squares mean	SE	Least squares mean	SE	
Lingual left	1.87	0.02	1.78	0.03	-4.60 0.0187*
Lingual right	1.88	0.03	1.83	0.03	-2.90 0.1587
Pericalcarine left	2.07	0.05	2.13	0.06	2.71 0.4871
Pericalcarine right	2.01	0.04	1.91	0.05	-4.99 0.1185
Cuneus left	2.16	0.04	2.24	0.05	4.03 0.1731
Cuneus right	2.08	0.03	2.07	0.03	-0.74 0.6998
Lateral occipital left	1.83	0.02	1.83	0.02	-0.20 0.8978
Lateral occipital right	1.84	0.02	1.78	0.02	-3.16 0.0143*
Cingulate cortex					
Rostral anterior cingulate left	2.23	0.05	2.23	0.05	-0.22 0.9424
Rostral anterior cingulate right	2.25	0.04	2.22	0.05	-1.54 0.5810
Caudal anterior cingulate left	2.11	0.03	2.10	0.04	-0.18 0.9375
Caudal anterior cingulate right	2.10	0.03	2.09	0.04	-0.64 0.7932
Posterior cingulate left	2.05	0.02	2.06	0.03	0.66 0.6983
Posterior cingulate right	2.11	0.02	2.04	0.02	-2.95 0.0414*
Isthmus cingulate left	2.06	0.03	2.08	0.04	1.05 0.6512
Isthmus cingulate right	2.04	0.03	2.09	0.04	2.62 0.2606
Insula cortex					
Insula left	2.03	0.02	1.98	0.02	-2.28 0.0996
Insula right	2.04	0.02	2.02	0.02	-1.01 0.4284

* $P < 0.05$

Table 4
Total surface area of infants at high genetic risk for schizophrenia and control infants

	Control infants		High-risk infants		Difference (%)	p values
	Least squares mean	Standard error (SE)	Least squares mean	Standard error (SE)		
Left hemisphere	400.36	6.89	394.97	7.80	-1.35	1
Right hemisphere	403.16	7.13	398.73	8.06	-1.10	0.684
Male left hemisphere	411.54	10.16	408.88	12.69	-0.65	0.870
Male right hemisphere	416.40	10.51	415.07	13.13	-0.32	0.937
Female left hemisphere	389.19	9.36	381.06	10.47	-2.09	0.555
Female right hemisphere	389.91	9.68	382.39	10.83	-1.93	0.598

Table 5
Regional cortical surface area of infants at high genetic risk for schizophrenia and control infants

Regions	Surface area (mm ²)		Difference (%)	p values		
	Control infants				High-risk infants	
	Least squares mean	SE			Least squares mean	SE
Frontal lobe						
Superior frontal left	3,298.75	65.25	3,331.75	73.83	1.00	0.7405
Superior frontal right	3,286.91	72.26	3,278.02	81.76	-0.27	0.9358
Rostral middle frontal left	2,692.28	62.90	2,588.08	71.17	-3.87	0.2781
Rostral middle frontal right	2,782.14	70.79	2,651.02	80.11	-4.71	0.2253
Caudal middle frontal left	974.64	26.69	947.43	30.20	-2.79	0.5044
Caudal middle frontal right	927.29	33.52	967.31	37.93	4.32	0.4345
Pars opercularis left	810.74	23.87	776.06	27.01	-4.28	0.3415
Pars opercularis right	648.46	16.74	660.68	18.94	1.88	0.6327
Pars triangularis left	613.61	17.16	622.41	19.42	1.43	0.7371
Pars triangularis right	751.32	20.28	683.22	22.94	-9.06	0.0279*
Pars orbitalis left	311.10	8.05	311.41	9.10	0.10	0.9800
Pars orbitalis right	404.95	13.12	385.32	14.85	-4.85	0.3273
Lateral orbital frontal left	1,091.76	24.40	1,100.49	27.60	0.80	0.8148
Lateral orbital frontal right	1,129.02	24.87	1,106.10	28.15	-2.03	0.5463
Medial orbital frontal left	793.58	17.81	779.79	20.16	-1.74	0.6124
Medial orbital frontal right	810.38	16.09	798.34	18.21	-1.49	0.6245
Frontal pole left	156.01	6.08	151.13	6.88	-3.13	0.5991
Frontal pole right	206.88	6.05	194.78	6.85	-5.85	0.1906
Precentral left	2,296.81	44.94	2,270.34	50.85	-1.15	0.6998
Precentral right	2,247.60	40.46	2,262.07	45.78	0.64	0.8149
Paracentral left	722.52	16.33	715.15	18.47	-1.02	0.7676
Paracentral right	834.91	17.89	804.01	20.24	-3.70	0.2580
Parietal lobe						
Postcentral left	2,093.44	37.16	2,058.70	42.05	-1.66	0.5404
Postcentral right	2,042.23	43.21	2,041.15	48.89	-0.05	0.9870

Regions	Surface area (mm ²)		Difference (%)		p values
	Control infants		High-risk infants		
	Least squares mean	SE	Least squares mean	SE	
Supramarginal left	1,870.70	43.31	1,900.53	49.01	1.59 0.6521
Supramarginal right	1,811.22	42.59	1,767.91	48.19	-2.39 0.5056
Superior parietal left	2,628.59	57.80	2,571.36	65.41	-2.18 0.5168
Superior parietal right	2,607.87	58.68	2,529.03	66.39	-3.02 0.3790
Inferior parietal left	2,116.89	58.49	2,130.92	66.18	0.66 0.8752
Inferior parietal right	2,489.18	59.35	2,622.34	67.16	5.35 0.1419
Precuneus left	1,980.17	46.03	1,932.89	52.09	-2.39 0.5014
Precuneus right	2,079.38	42.65	2,003.64	48.26	-3.64 0.2449
Temporal lobe					
Superior temporal left	1,789.68	35.55	1,779.82	40.23	-0.55 0.8559
Superior temporal right	1,778.61	37.09	1,796.56	41.96	1.01 0.7514
Middle temporal left	1,395.79	33.51	1,393.71	37.92	-0.15 0.9675
Middle temporal right	1,549.05	38.91	1,520.36	44.03	-1.85 0.6293
Inferior temporal left	1,416.77	35.09	1,373.06	39.70	-3.09 0.4147
Inferior temporal right	1,327.43	29.23	1,287.46	33.07	-3.01 0.3707
Transverse temporal left	262.81	7.43	249.74	8.40	-4.97 0.2492
Transverse temporal right	183.02	6.74	184.16	7.62	0.63 0.9113
Banks superior temporal sulcus left	399.37	13.60	395.81	15.39	-0.89 0.8638
Banks superior temporal sulcus right	365.03	10.23	383.97	11.58	5.19 0.2255
Entorhinal left	244.68	7.16	244.03	8.10	-0.26 0.9529
Entorhinal right	239.91	6.87	224.22	7.78	-6.54 0.1351
Parahippocampal Left	334.07	7.44	323.59	8.41	-3.14 0.3563
Parahippocampal Right	279.71	5.87	268.22	6.65	-4.11 0.2005
Temporal pole left	331.95	10.59	342.26	11.98	3.11 0.5238
Temporal pole right	329.90	8.76	320.62	9.92	-2.81 0.4884
Fusiform left	1,448.50	33.85	1,406.88	38.30	-2.87 0.4208
Fusiform right	1,382.46	31.45	1,349.95	35.59	-2.35 0.4985
Occipital lobe					
Lingual left	1,452.72	37.70	1,455.59	42.66	0.20 0.9,604

Regions	Surface area (mm ²)		Difference (%)		<i>p</i> values
	Control infants		High-risk infants		
	Least squares mean	SE	Least squares mean	SE	
Lingual right	1,391.84	36.77	1,390.34	41.61	-0.11 0.9786
Pericalcarine left	522.03	18.08	521.05	20.46	-0.19 0.9718
Pericalcarine right	591.92	25.21	620.09	28.52	4.76 0.4644
Cuneus left	727.69	20.70	711.33	23.42	-2.25 0.6048
Cuneus right	775.02	18.70	775.48	21.16	0.06 0.9871
Lateral occipital left	2,292.95	45.00	2,205.78	50.91	-3.80 0.2047
Lateral occipital right	2,219.25	49.16	2,196.34	55.62	-1.03 0.7603
Cingulate cortex					
Rostral anterior cingulate left	291.72	9.60	271.99	10.86	-6.76 0.1783
Rostral anterior cingulate right	222.05	9.43	209.75	10.67	-5.54 0.3927
Caudal anterior cingulate left	223.69	8.97	228.58	10.15	2.18 0.7215
Caudal anterior cingulate right	258.48	7.30	260.70	8.26	0.86 0.8418
Posterior cingulate left	533.00	11.88	512.23	13.44	-3.90 0.2523
Posterior cingulate right	518.66	15.86	499.98	17.95	-3.60 0.4408
Isthmus cingulate left	377.09	8.59	378.21	9.72	0.30 0.9320
Isthmus cingulate right	341.64	8.88	339.30	10.05	-0.68 0.8633
Insula cortex					
Insula left	1,025.53	17.71	1,018.13	20.03	-0.72 0.7843
Insula right	981.57	16.45	979.60	18.62	-0.20 0.9376

* *p* < 0.05